Bulletin of The Faculty of Psychological & Physical Science, No. 14, 23–31, 2018

An Elementary Theory of a Dynamic Weighted Digraph (1)

Naohito CHINO*

Abstract

This paper is the first part of the revised version of my handout presented elsewhere (Chino, 2018). In this theory we assume that the weight matrix denotes the proximity strengths among nodes at any instant of time, and that it varies as time proceeds. Then, applying the Hermitian Form model proposed by Chino and Shiraiwa (1993), we get the configuration of nodes at any instant of time in a p-dimensional Hilbert space, H^p, or an indefinite space. For simplicity, we assume that p=1 in this paper. Then, we have the correspondence among digraph, its weight matrix, and the configuration of nodes in a one-dimensional Hilbert space, H. The purpose of our theory is to classify elementary patterns of changes in digraphs (thus, in its weight matrices as well as in the corresponding configurations) over time, by assuming that there exists a latent process which governs these changes in the configurations of nodes, which can be described by a set of complex nonlinear difference equations in H^p in the most general case. We first revisit such patterns of changes in digraphs in the case when p=1 and the difference equation is linear, which are shown elsewhere (Chino, 2017a, b; Chino, 2018). Our major results in this paper are concerned with these patterns in the case when the difference equation is quadratic. The quadratic system as well as its transformed quadratic system exhibit interesting chaotic behaviors under certain mild conditions. Relations of such behaviors to the random walk as well as the Brownian motion are discussed.

Keywords: complex difference equation, Hilbert space, Chino-Shiraiwa theorem, dynamic weighted digraph, chaos, trade imbalance, neural network.

1. Introduction

Let us imagine a special matrix, $W_3 = \begin{pmatrix} 8 & 1 & 6 \\ 3 & 5 & 7 \\ 4 & 9 & 2 \end{pmatrix}$. It is an example of the *magic square* of order 3. If we consider the matrix as the weight matrix associated with a digraph, we can draw the digraph as follows, using, for example, MATLAB:

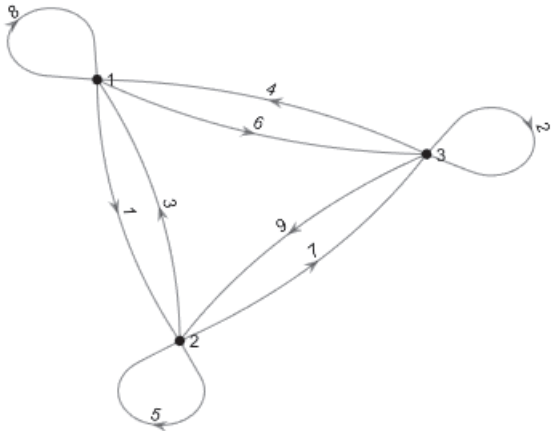

Figure 1. The digraph associated with the weight matrix W_3.

As is well known, the weighted digraph is a digraph with weights specified at time *n*, which are attached to each *directed arc* (or edge, link) between *nodes* (or vertices) as well as each *loop* of the digraph. In asymmetric MDS, nodes correspond to members of a group, while weights attached to directed arcs correspond to the proximities among objects.

Our elementary theory of a *dynamic weighted digraph* assumes that the weight matrix denotes the *proximity strengths* among nodes at any instant of time, and that it varies as time proceeds. If we apply HFM (the Hermitian

*Department of Psychology, Faculty of Psychological & Physical Science, Aichi Gakuin University.
Requests for reprints should be sent to: chino@dpc.agu.ac.jp

This is the first part of the revised version of my handout titled "An elementary theory of a dynamic weighted digraph" presented at *the 46th annual meeting of the Behaviormet-ric Society of Japan*, Tokyo, Japan.

Form Model) (Chino & Shiraiwa, 1993) to the weight matrix, then we obtain the configuration of objects (nodes) at any instant of time in a *p-dimensional Hilbert space*, H^p or an indefinite metric space.

Our theory assumes that the *Hermitian matrix* corresponding to the weight matrix is *positive semi-definite*, in the most general case and its weights are measured at a ratio level. Then, we have the correspondence among digraph, weight matrix, and configuration of objects (nodes) at any instant of time:

digraph ⇔ weight matrix ⇔ configuration of nodes in H^p

As a result, changes in digraphs over time are considered as changes in configurations of nodes in H^p over time. In this paper we shall assume that p is one, that is, a *one*-dimensional Hilbert space, H.

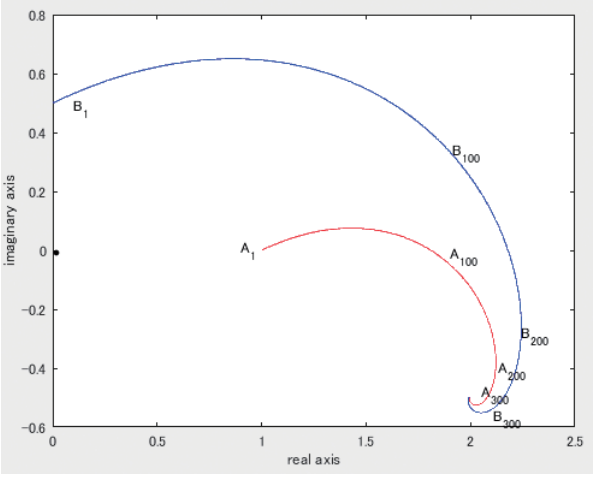

Figure 2. Trajectories of two members j (=A) and k (=B) on the complex plane in the special case when $a_{jk} = .001(1 + i)$, $a_{kj} = -0.02(1 + i)$. This figure was reproduced from Figure 2–3 in Chino (2017a) as well as Figure 7 in Chino (2018).

Let us now look at some of the literature which deals with the dynamical changes in digraphs over time. It can be divided into two categories, one using the *differential equation model* and the other the *difference equation model*. For example, McCann et al. (1998) proposed an interesting *nonlinear differential equation model* as a food-web model, in which they considered food-webs composed of three or four species, one being the top predator, another being a resource species, and the other being one or two consumer species. They examined the effects of interaction strengths on changes in densities of species over time. Interaction strengths are bifurcation parameters of their model. Results indicated that chaotic behaviors occur when the (relative) interaction strength takes below some value in a food web with multiple intermediate consumers.

Chesson and Warner (1981) proposed a lottery model which is described by a set of *nonlinear difference equations*. This model explains a certain coexistence phenomenon of species. However, these models merely deal with changes in numbers or density of species. Moreover, most of the network models proposed previously assume that the state space of the system is *real*, except for the complex neural network models.

In contrast, our elementary theory of dynamic digraph then assumes that these changes in configurations of nodes can be described by a set of complex nonlinear differ-rence equations in H^p in the most general case. The purpose of our theory is to classify elementary patterns of changes in digraphs over time, by assuming that there exists a latent process which governs these changes in digraph, which can be described by a set of complex nonlinear difference equations in H^p.

2. Elementary theory of dynamic weighted digraph

We describe the changes in N nodes over time by the following *set of complex difference equations in a Hilbert space*, H^p:

$$\boldsymbol{z}_{j,n+1} = \boldsymbol{z}_{j,n} + \sum_{m=1}^{q} \sum_{k \neq j}^{N} \boldsymbol{D}_{jk}^{(m)} \boldsymbol{f}^{(m)}\left(\boldsymbol{z}_{j,n} - \boldsymbol{z}_{k,n}\right) + \boldsymbol{g}\left(\boldsymbol{u}_{j,n}\right) + \boldsymbol{z}_0, \quad (1)$$

where j and k range from *1* to N, i.e., the number of nodes, and n indicates the iteration number. This means that the coordinate of node j at $(n+1)$th iteration in H is assumed to be generated by node j at nth iteration plus the qth order polynomial of the difference between those of node j and node k at nth iteration, where k ranges from *1* to N except j.

Moreover, $\boldsymbol{D}_{jk}^{(m)} = diag\left(\alpha_{jk}^{(1,m)}, \alpha_{jk}^{(2,m)}, \ldots, \alpha_{jk}^{(p,m)}\right)$ is the coefficient matrix of Eq. (1). It is related to the *mutual interaction matrix* among nodes, which determines the displacements of nodes in a latent space H^p, as shown below. We assume that this matrix is constant over time. In any case, Eq. (1) assumes that the force acting on each of the nodes in H^p is a polynomial function of the differences in coordinates between one node and the other nodes in the space.

This equation should be contrasted with Newton's second law of motion, i.e., $\boldsymbol{F}=m\boldsymbol{a}$, in that the force exerting on a celestial body is proportional to the second derivatives of it's coordinates in the Euclidean space, E^3, with respect to time. The force assumed by Eq. (1) might possibly be applied to international trade systems, neural network systems, interorgan communication network systems, social network

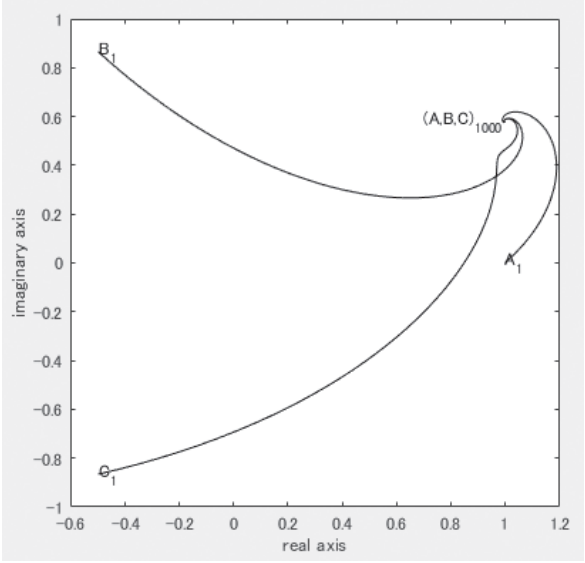

Figure 3. Trajectories of Eq. (5) with a special case of $\boldsymbol{A}_3$. This figure was reproduced from Figure 7–4 in Chino (2017a) as well as Figure 11 in Chino (2018).

systems, and so on.

The purpose of our elementary theory is two-fold. One is *theoretical*, and the other *practical*. For theoretical purposes, we compute the trajectories of nodes using Eq. (1) with a mutual interaction matrix, by setting an arbitrary initial configuration of nodes. Then, we classify the patterns of changes in digraphs over time according to the patterns of trajectories of nodes over time.

For practical purposes, we may first observe a proximity matrix at an instant of time as the initial weight matrix of digraph under study.

In Chino (2017a, b), we showed some theoretical results of our difference equation model described by Eq. (1) in the cases when p=1 and m=1, and N=2, i.e., the dyadic case:

In this case, Eq. (1) becomes

$$\begin{cases} z_{j,n+1} = z_{jn} + \alpha_{jk}(z_{jn} - z_{kn}) \\ z_{k,n+1} = z_{kn} + \alpha_{kj}(z_{kn} - z_{jn}) \end{cases}. \tag{2}$$

If we use the vector notations, e.g., $\boldsymbol{z}_n = (z_{jn}, z_{kn})^t$, then Eq. (2) has a simple expression,

$$\boldsymbol{z}_{n+1} = \boldsymbol{A}_2\boldsymbol{z}_n, \quad \text{where} \quad \boldsymbol{A}_2 = \begin{pmatrix} 1+\alpha_{jk} & -\alpha_{jk} \\ -\alpha_{kj} & 1+\alpha_{kj} \end{pmatrix}, \tag{3}$$

and we call $\boldsymbol{A}_2$ as the mutual interaction matrix in the dyadic case. The eigenvalues of $\boldsymbol{A}_2$ are $1 + a_{jk} + a_{kj}$ and 1.

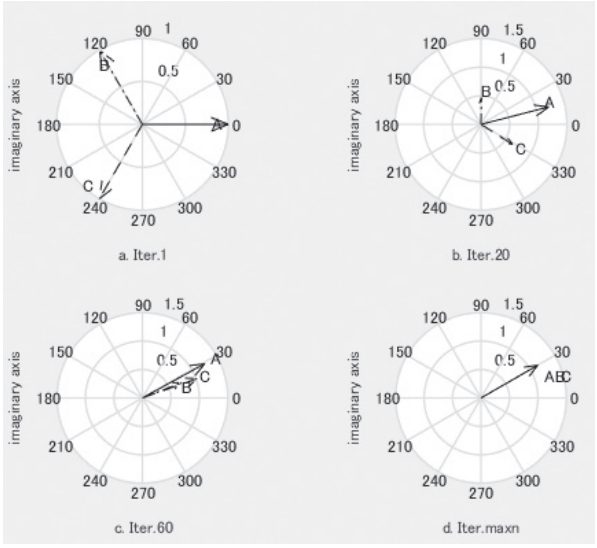

Figure 4. Configurations of nodes as snapshots of their trajectories.

Similarly, if p=1, m=1, and N=3, i.e., the triadic case, then Eq. (2) can be written as

$$\begin{cases} z_{j,n+1} = z_{jn} + \alpha_{jk}(z_{jn} - z_{kn}) + \alpha_{jl}(z_{jn} - z_{ln}) \\ z_{k,n+1} = z_{kn} + \alpha_{kl}(z_{kn} - z_{ln}) + \alpha_{kj}(z_{kn} - z_{jn}) \\ z_{l,n+1} = z_{ln} + \alpha_{lj}(z_{ln} - z_{jn}) + \alpha_{lk}(z_{ln} - z_{kn}) \end{cases}. \tag{4}$$

If we denote the mutual interaction matrix in the triadic case as $\boldsymbol{A}_3$, and if we use $\boldsymbol{z}_n = (z_{jn}, z_{kn}, z_{ln})^t$, then we have

$$\boldsymbol{z}_{n+1} = \boldsymbol{A}_3\boldsymbol{z}_n, \tag{5}$$

where $\boldsymbol{A_3} = \begin{pmatrix} 1+\alpha_{jk}+\alpha_{jl} & -\alpha_{jk} & -\alpha_{jl} \\ -\alpha_{kj} & 1+\alpha_{kl}+\alpha_{kj} & -\alpha_{kl} \\ -\alpha_{lj} & -\alpha_{lk} & 1+\alpha_{lj}+\alpha_{lk} \end{pmatrix}$.

Matrices $\boldsymbol{A}_2$ and $\boldsymbol{A}_3$ are considered as special cases of the *mutual interaction matrices* of our model. As pointed out in Chino (2017a, b; 2018), patterns of *eigenvalues* in these matrices determine the patterns of trajectories of nodes over time.

For example, dynamical scenarios of the solution curve of the dyadic linear difference equation described by Eq. (3) have three patterns depending on the absolute value of the eigenvalue, $1 + a_{jk} + a_{kj}$, as follows (Chino, 2017):

$$\begin{cases} diverge, & if\ |1+\alpha_{jk}+\alpha_{kj}| > 1 \\ diverge\ in\ lines, & if\ |1+\alpha_{jk}+\alpha_{kj}| = 1 \\ converge, & if\ |1+\alpha_{jk}+\alpha_{kj}| < 1 \end{cases}.$$

Figure 2 shows the trajectories of two members (nodes) in H in the special case when the solution curves converge.

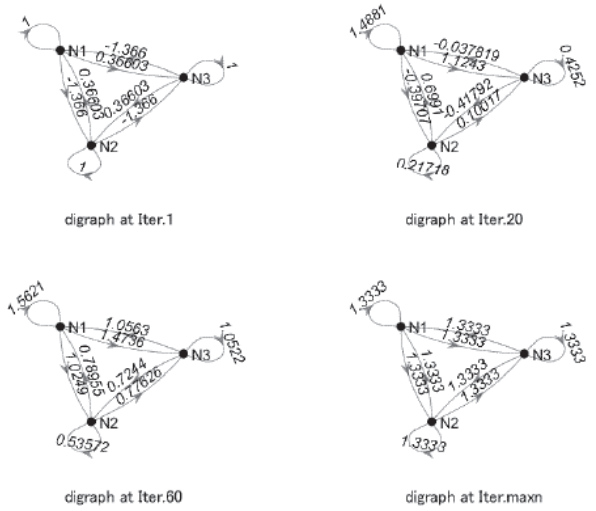

Figure 5. Digraphs reproduced from the trajectories of Fig. 2.

Similarly, dynamical scenarios of the solution curve of the triadic linear difference equation described by Eq. (5) have roughly four patterns depending on the two eigenvalues, λ_2, λ_3, except $\lambda_1 = 1$. The two eigenvalues, λ_2, λ_3, can be written as

$$1 + \frac{1}{2}\sum_{g\neq h}^{3}\sum_{h}^{3}\alpha_{gh} \pm \sqrt{D},$$

and determine the patterns of trajectories, where D is a special quadratic function of a_{gh}'s.

Fig. 3 shows the trajectories of Eq. (5) with a special case of $\boldsymbol{A}_3$, where

$$\boldsymbol{A}_3 = \begin{pmatrix} 1, & 0.01(1-i), & -0.01(1-i) \\ 0.02(1-i), & 1, & -0.01(1-i) \\ 0.02(1-i), & 0.02(1-i), & 1 \end{pmatrix}. \quad (6)$$

Here, the initial configuration of nodes is assumed to be a *tripartite deadlock*. Since the eigenvalues of this matrix are 1.0, 0.98+0.02i, 0.97+0.03i, all the trajectories of this system converge to a point (i.e., 1+0.5774i in H^1), as depicted in Fig. 3.

If we take snapshots of the three nodes on the trajectories in Fig. 3 at times, say, n=1, 20, 60, 1000, we have the configurations of nodes at these times. Fig. 4 shows them.

If we reproduce the weight matrices at time, n=1, 20, 60, 1000 from the configurations shown above, the corresponding digraphs can be drawn. To do this job, we may apply the formula which connects the proximity from node j to node k with the coordinates of nodes in the p-dimensional Hilbert space. That is,

$$s_{jk} = -\frac{1}{2}\left\{\|\boldsymbol{v_j} - \boldsymbol{v_k}\|^2 + \|\boldsymbol{v_j} - i\boldsymbol{v_k}\|^2\right\} + \left(\|\boldsymbol{v_j}\|^2 + \|\boldsymbol{v_k}\|^2\right). \quad (7)$$

Here, the proximity s_{jk} is real and equals W_{jk}, while the coordinates of nodes, $\boldsymbol{v_j}$ is complex and equals Z_j in this context in HFM (Chino & Shiraiwa, 1993).

We show the corresponding digraphs in Fig. 5. It should be noticed that not only the self-proximities of nodes but also the proximities among nodes are the same values at the last iteration. Such a result can be confirmed by applying Eq. (7) to the case where $\boldsymbol{v_j} = \boldsymbol{v_k}$.

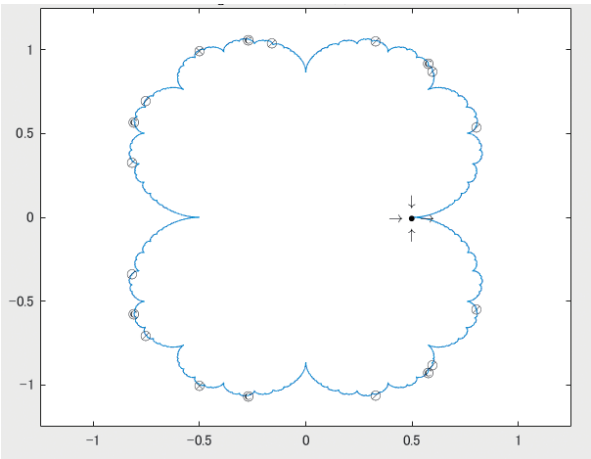

Figure 6. Julia set for $Z_{jk,n+1} = Z_{jk,n}^2 + 0.25$ with a *parabolic fixed point* (0.5), two repelling periodic points of period 2 ($-0.5 \pm i$), and six repelling periodic points of period 3 with the © mark, and twelve repelling periodic points of three 4-sycles. This figure was reproduced from Figure 11–1 in Chino (2017a) as well as Figure 1 in Chino (2018).

3. Dynamic weighted digraph when the latent dynamics have quadratic terms

In Chino (2017a, 2018), we discussed a bit about our difference equation model described by Eq. (1) when N=2, and q=2, i.e.,

$$\begin{cases} z_{j,n+1} = z_{jn} + \alpha_{jk}^{(1)}(z_{jn} - z_{kn}) + \alpha_{jk}^{(2)}(z_{jn} - z_{kn})^2, \\ z_{k,n+1} = z_{kn} + \alpha_{kj}^{(1)}(z_{kn} - z_{jn}) + \alpha_{kj}^{(2)}(z_{kn} - z_{jn})^2. \end{cases} \quad (8)$$

As discussed there, this type of system has a very desirable property in that we can utilize the heritage of the theory of the complex dynamical system developed in mathematics directly in classifying its trajectories. In fact, defining a new variable, $u_{jkn} = z_{jn} - z_{kn}$, and transforming it linearly, we have a new system

$$Z_{jk,n+1} = Z_{jk,n}^2 + \gamma_{jk}^{(1)}, \quad (9)$$

where $\gamma_{jk}^{(1)} = \frac{1}{2}\beta_{jk}^{(1)} - \frac{1}{4}\left[\beta_{jk}^{(1)}\right]^2$, and $\beta_{jk}^{(1)} = 1 + \alpha_{jk}^{(1)} + \alpha_{kj}^{(1)}$. Depending on the value of $\gamma_{jk}^{(1)}$, we have the *Mandelbrot set* (Mandelbrot, 1977).

For example, in the case when $\gamma_{jk}^{(1)} = 0.25$, that is, $Z_{jk,n+1} = Z_{jk,n}^2 + 0.25$, this equation is contained in the

Mandelbrot set, and the corresponding trajectory is known as the "*cauliflower set*", which is shown in Fig. 6.

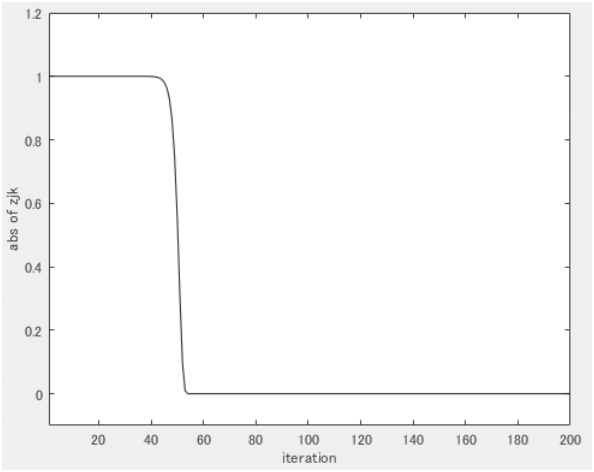

Figure 7. Change in absolute value of the linearized system, $Z_{jk,n+1} = {Z_{jk,n}}^2$ with $Z_{jk,1} = i$ in C.

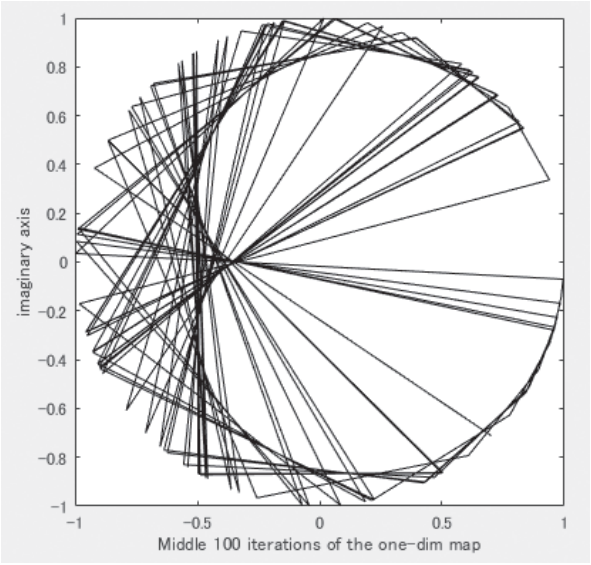

Figure 8. Revised trajectory with initial value i in C after 100 iterations.

As pointed in Chino (2017a, 2018), we can utilize various theoretical results established in the complex dynamical system, in examining the dynamical scenarios of Z_{jkn}. Some of the key phrases in these results are the fixed point as well as the periodic point (orbit), the multiplier of these points, and the Fatou set and Julia set (e.g., Carleson & Gamelin, 1993).

First, the fixed point and the multiplier of these points are defined as follows:

Suppose f is a *holomorphic function*, that is, an analytic function in a complex space. Then, z_f is called a *fixed point* if $f(z_f) = z_f$. The number $\lambda = f'(z_f)$ is called the *multiplier* of the fixed point. Here, f′is the first derivative of f with respect to z_f.

Second, the *multiplier* determines the property of the fixed point as follows (e.g., Carleson & Gamelin, 1993, p. 27):

(1) *Attracting* if $|\lambda| < 1$. (If $\lambda = 0$, we refer to a *superattracting* fixed point.)
(2) *Repelling* if $|\lambda| > 1$.
(3) *Rationally neutral* if $|\lambda| = 1$ and $\lambda^n = 1$ for some integer n.
(4) *Irrationally neutral* if $|\lambda| = 1$ but λ^n is never 1.

Here, function f in the case of the Mandelbrot set is described as follows:

$$f(z) = z^2 + c, \tag{10}$$

Third, the periodic point and the multiplier of these points are defined as follows (e.g., Milnor, 2000):

A *periodic orbit* or "cycle" is the function such that

$$f: z_0 \mapsto z_1 \mapsto \cdots \mapsto z_{m-1} \mapsto z_m = z_0, \tag{11}$$

for a holomorphic map. Then, the multiplier λ of the orbit is the first derivative of the m-fold iterate $f^{\circ m}$ at a point of the orbit, and

$$\lambda = \left(f^{\circ m}\right)'^{(z_i)} = f'(z_1) \cdot f'(z_2) \cdot \ldots \cdot f'(z_m) \cdot \tag{12}$$

In the case of cauliflower set, c equals 0.25, and thus several points on the Julia set are identified as *parabolic fixed points*, repelling periodic points of period 2, and repelling periodic points of period 3, which are shown in Fig. 6.

At this point, it should be noticed that the major concern of the complex dynamical system is to examine the local qualitative behaviors of the fixed points and periodic points of the system under consideration, using the multipliers of these special points. In contrast, the major concern of our complex difference systems is to examine not only the local qualitative behaviors of the fixed points as well as the periodic points but also the global qualitative behaviors of nodes in H. This means that even in the dyadic system described by Eq. (8), we must examine not only the local qualitative behaviors of the linearly transformed variable $Z_{jk,n}$ in Eq. (9) but also the global qualitative behaviors of the original dyadic system described by Eq. (8).

One method to do the latter job may be to compute the Lyapunov exponent of the dyadic system. We began the simulation study of the dyadic system whose qualitative behaviors of the linearized system described by Eq. (9) are simple. Such a linearized system may be the system such that $\gamma_{jk}^{(1)} = 0$ in Eq. (9). To attain this value, we set the α′s

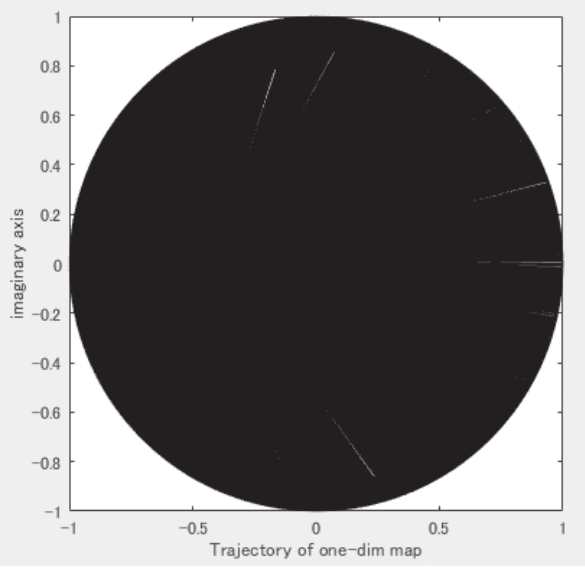

Figure 9. Revised trajectory with initial value i in C after100 iterations.

as $\alpha_{jk}^{(1)} = 0.9564i$, $\alpha_{kj}^{(1)} = -1 - 0.9564i$, $\alpha_{jk}^{(2)} = 0.01$, and $\alpha_{kj}^{(2)} = 1.5375 - 0.9564i$.

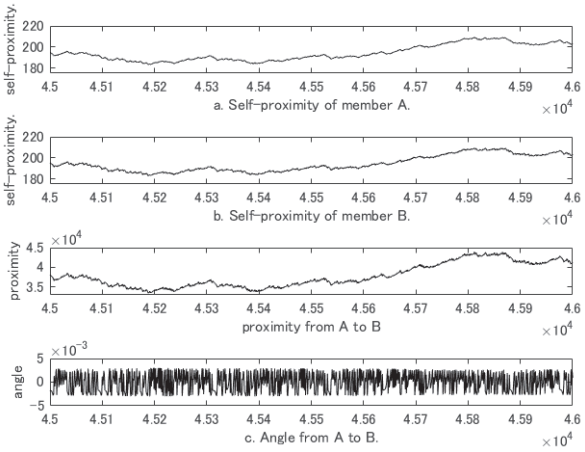

Figure 10. Trajectories of four indices of the original dyadic system. 10-a and 10-b are those of node j (member A) and node k (member B), respectively. 10-c is the trajectory of the proximity from node j to node k. 10-d is the trajectory of the angle from node j to node k.

It is well known that the Julia set of this system is the unit circle with origin 0 in C (equivalently, H), where C is the complex plane. Moreover, it is easy to show that this system has two fixed points, 1 and 0 (the origin), and these points are repelling and superattracting, respectively. As a result, when we start from an arbitrary point on the unit circle, the trajectory moves chaotically on the circle, at least theoretically. (Notice that this circle is not a fractal since the unit circle is not self-similar.) As a trial, we set the initial value of this system as *i on the unit circle* in C, since this point is not the fixed point of the system.

However, due to the rounding errors of computer, which is an inevitable phenomenon even if we specify a long fixed-decimal format, the trajectory with initial value i runs off the unit circle within no greater than, say, 50 iterations. Fig. 7 shows this.

In such a case, however, we can revise the trajectory, because the unit circle as a Julia set has an explicit mathematical expression. That is, every time when the trajectory runs off the unit circle, we may put it back on the unit circle. Then, the trajectory remains the unit circle. Fig. 8 shows the revised trajectory after 100 iterations, while Fig. 9 depicts it after 10,000 iterations. The trajectory in Fig. 9 almost fills out the unit disk chaotically after 10,000 iterations.

Of course, the strict Lyapunov exponent of this one-dimensional system, $Z_{jk,\,n+1} = Z_{jk,\,n}{}^2$, is $\lambda = ln\,2 = 0.69314718\ldots$, thus the system has chaos.

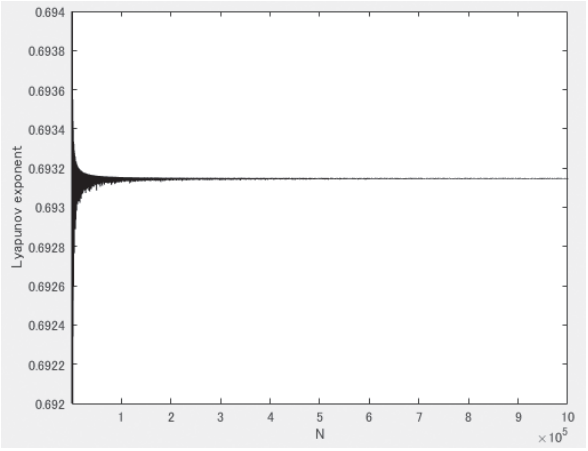

Figure 11. The largest Lyapunov exponent of the original two dimensional system.

Next, we shall proceed to examine qualitative behaviors of the original dyadic system described by Eq. (8).

First, we computed the largest Lyapunov exponent of this dyadic system. Fig. 11 shows it. It converges to 0.693147148…, which is very close to that of the linearized system $Z_{jk,\,n+1} = Z_{jk,\,n}{}^2$ discussed above. This result clearly shows that the dyadic system has chaos.

Second, we shall zoom up trajectories shown in Fig. 10 to examine further the features of these trajectories. For example, Fig. 12 shows the expanded trajectories of the proximity from A to B (or j to k) from iteration 45,000 to 46,000. This trajectory is reminiscent of one-dimensional random walk or Brownian motion (Brown, 1828).

Third, we show trajectories of the dyadic system after 50,000 iterations. Figs. 13 and 14 shows those of node *j* and *k*, respectively.

In contrast, Fig. 15 shows the simultaneous plot of the trajectories depicted in Figs. 13 and 14 using different colors, yellow and black.

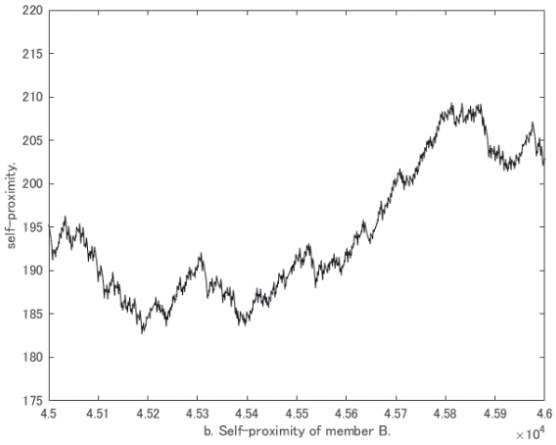

Figure 12. Expanded trajectories of 10-c from iteration 45,000 to 46,000.

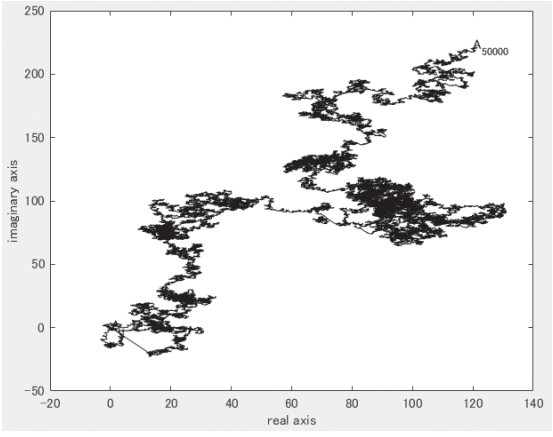

Figure 13. Trajectory of the node *j* after 50,000 iterations.

Fig. 15 shows that the trajectories of two nodes are very close to each other. This point may be contrasted with the usual random work as well as the Brownian motion.

To compare the trajectories of our dyadic system with those of the random walk and the Brownian motion, we draw Figs. 16 and 17, which are trajectories of a simple random walk and a Brownian motion, both on the x-axis.

Figs. 18 and 19 are trajectories of a two-dimensional random walk and a planar Brownian motion after 20,000 iterations.

It is interesting to note that trajectories of our special dyadic system are reminiscent of the random walk or the

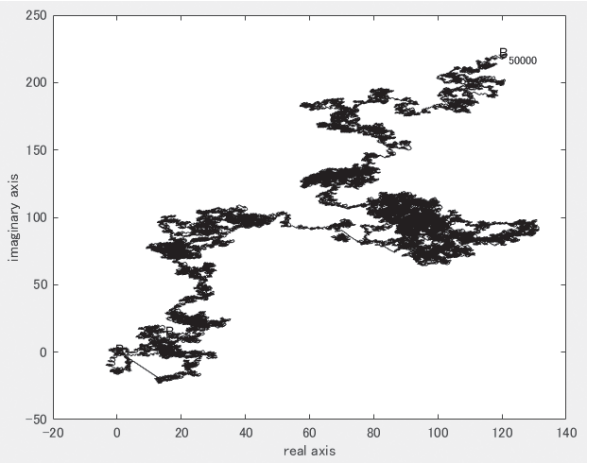

Figure 14. Trajectory of the node *k* after 50,000 iterations.

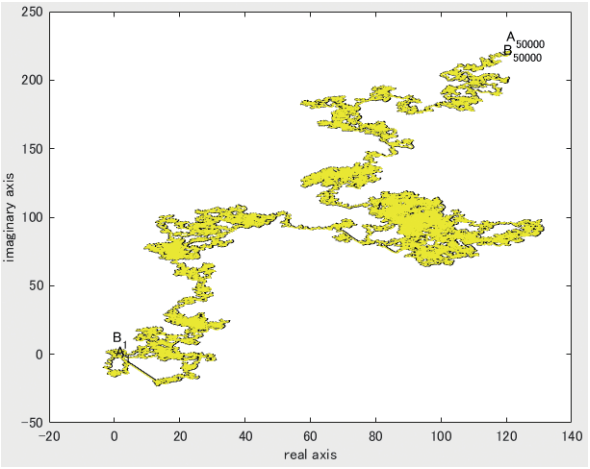

Figure 15. Simultaneous plot of the two trajectories shown in Figs. 13 and 14.

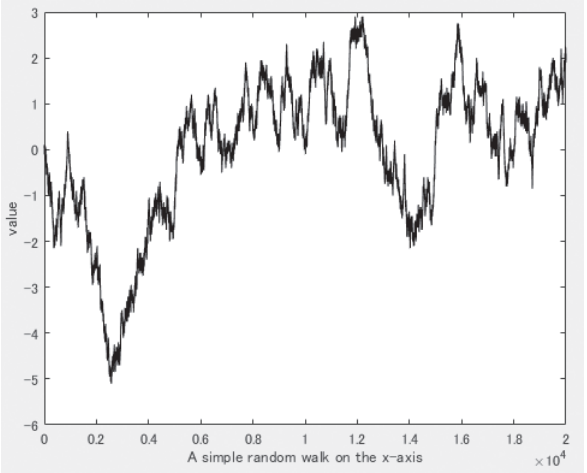

Figure 16. Trajectories of a simple random walk on the x-axis.

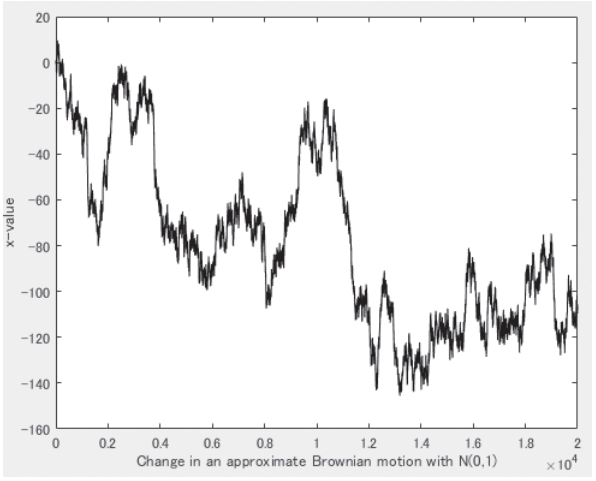

Figure 17. Trajectory of a planar Brownian Motion after 20000 iterations.

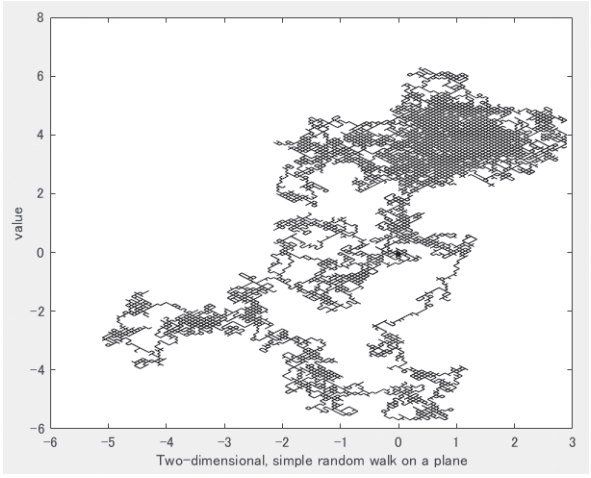

Figure 18. Two-dimensional simple random walk after 20000 iterations.

Brownian motion.

4. Conclusion

In this paper we propose an elementary theory of a dynamical weighted digraph. In this theory we first assume that the weight matrix denotes the proximity strengths among nodes at any instant of time, and that it varies as time proceeds. Then we apply HFM (the Hermitian Form Model) (Chino & Shiraiwa, 1993) to the weight matrix, and obtain the configuration of objects (nodes) at any instant of time in a p-dimensional Hilbert space, H^p or an indefinite metric space. Here, we assume that the *Hermitian matrix* corresponding to the weight matrix is *positive semi-definite*, in the most general case and its weights are measured at a ratio level. Then, we have the correspondence among digraph, weight matrix, and configuration of objects (nodes) at any instant of time. As a result, changes in digraphs over time are considered as changes in configurations of nodes in H^p over time.

Our elementary theory of dynamic digraph then assumes that these changes in configurations of nodes can be described by a set of complex nonlinear difference equations in H^p in the most general case. The purpose of our theory is to classify elementary patterns of changes in digraphs over time, by assuming that there exists a latent process which governs these changes in digraph, which can be described by a set of complex nonlinear difference equations in H^p.

In this paper, we restrict the dimension p of the state space to one, and conducted some simulation studies in order to classify elementary patterns of changes in digraphs over time. It is easy to show that such patterns can be enu-

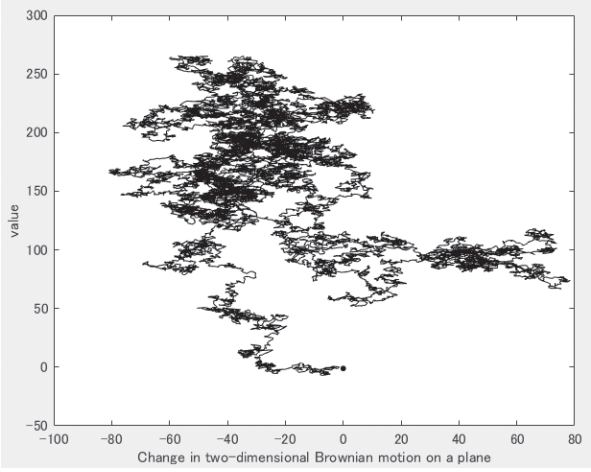

Figure 19. Planar Brownian motion after 20000 iterations.

merated simply in the case when the latent dynamics are linear (Chino, 2017a, b; Chino, 2018). Our major results in this paper are concerned with the patterns in the case when the latent dynamics have quadratic terms especially in the case where N=2 and q=2 in Eq. (1), i.e., Eq. (8). As discussed elsewhere (Chino, 2017a, 2018), this type of system has a very desirable property in that we can utilize the heritage of the theory of the complex dynamical system developed in mathematics directly in classifying its trajectories.

In fact, the transformed new system of Eq. (8), i.e., Eq. (9) becomes the Mandelbrot set (Mandelbrot, 197) in some cases. Furthermore, the original quadratic system, Eq. (8) also exhibits *chaotic behaviors* which are very similar to the random work or the Brownian motion. Moreover, analyses of the first three quantities of Fig. 10 by the Higuchi's method (Higuchi, 1988) clearly show that these quantities

have the characteristic of *fractal*.

Acknowledgements

The author is indebted to Gregory L. Rohe for proofreading of an earlier version of this paper.

References

Bang-Jensen, J. & Guttin, G. (2007). *Digraphs—Theory, Algorithms and Applications*. New York: Springer-Verlag.

Brown, R. (1828). A brief account of microscopical observations made in the months of June, July, and August, 1827 on the particles contain-ed in the pollen of plants; and on the general existence of active molecules in organic and inorganic bodies.
http://sciweb.nybg.org/science2/pdfs/Brownian.pdf.

Carlesson, L. & Gamelin, T. W. (1993). Complex dynamics, New York: Springer-Verlag.

Chino, N. (2017a). Dynamical scenarios of changes in asymmetric relationships on a Hil-bert space. Proceedings of the 45th Annual Meeting of the Behaviormetric Society, September 1, Shizuoka, Japan.

Chino, N. (2017b). Dynamical scenarios of changes in asymmetric relationships over time (1). *Bulletin of The Faculty of Psychological & Physical Science*, **13**, 23–31.

Chino, N. (2018). Dynamical scenarios of changes in asymmetric relationships over time (2). *Journal of the Institute for Psychological and Physical Science*, **10**, 7–14.

Chino, N. & Shiraiwa, K. (1993). Geometrical structures of some non-distance models for asymmetric MDS. *Behaviormetrika*, **20**, 35–4.

Elaydi, S. N. (2000). *An introduction to difference equations*. New York: Springer-Verlag.

Higuchi, T. (1988). Approach to an irregular time series on the basis of the fractal theory. *Physica D*, **31**, 277–283.

McCann, K., & Hastings, A. & Huxel, G. R. (1998). Weak trophic interactions and the balance of nature. *Nature*, **395**, 794–798.

Milnor, J. (2000). *Dynamics in one dimensional complex variable*. Braunschweig: Vieweg.

(Final version submitted on September 28, 2018)